

Supporting Information

Highly Efficient Atom Transfer Radical Polymerization System Based on the SaBOX/Copper Catalyst

Zhi-Hao Chen,^{†,‡,#} Xiao-Yan Wang,^{*,†} Xiu-Li Sun,^{†,§} Jun-Fang Li,[†] Ben-Hu Zhu,[†] and Yong Tang^{*,†}

[†]State Key Laboratory of Organometallic Chemistry, Shanghai Institute of Organic Chemistry, Chinese Academy of Sciences, 345 Lingling Lu, Shanghai 200032, China

[‡]School of Physical Science and Technology, ShanghaiTech University, 393 Middle Huaxia Road, Shanghai 201210, China

[#]University of Chinese Academy of Sciences, No.19(A) Yuquan Road, Beijing 100049, China

[§]CAS Key Laboratory of Energy Regulation Materials, Shanghai Institute of Organic Chemistry, Chinese Academy of Sciences, 345 Lingling Lu, Shanghai 200032, China

*E-mail: wangxiaoyan@sioc.ac.cn; tangy@sioc.ac.cn

Contents

1. General Information	S3
2. General ATRP Procedure	S5
3. The SARA ATRP of MMA Employing Different Ligands and Initiators.....	S6
4. The SARA ATRP of MMA with $DP_{\text{target}} = 100$ in IPA/DMSO Mixed Solvent.....	S6
5. First-Order Kinetic Plots as well as Evolution of MW and Đ as a Function of Monomer Conversion for ATRP of MMA.....	S7
6. The GPC Traces of PMMA with Different DP_{target} s.....	S8
7. MALDI-TOF Mass Spectrum of PMMA.....	S8
8. In Situ Chain Extension Experiments.....	S9
9. The Determinations of Equilibrium Constant and Activation Rate Constant.....	S10

1. General Information

Unless stated otherwise, all manipulations with air- and moisture-sensitive chemicals and reagents were performed using standard Schlenk techniques on a dual-manifold line, or in an inert gas (N₂)-filled glovebox. All solvents and reagents were obtained from commercial sources and were purified according to standard procedures before use. All the monomers were purchased and dried over activated CaH₂ overnight, followed by vacuum distillation and stored in bottles at -22 °C inside of a freezer. ¹H NMR spectra were recorded on Varian 400 MHz spectrometer and Agilent Technologies 400 MHz spectrometer. The number-average molecular weight (M_n) and polydispersity index (\mathcal{D}) were measured by gel permeation chromatography (GPC). The analysis was undertaken at 25 °C with purified high-performance-liquid-chromatography-grade THF (for polymers of acrylate, methacrylate and styrene type monomers) or DMF (for poly(N,N-dimethylacrylamide)) or water (for poly(methacrylic acid)) as the eluent. Calibration was performed with standard PMMA (for polymers of acrylates and methacrylates as well as poly(N,N-dimethylacrylamide)), PS (for polymers of styrene type monomers) or PEG (for poly(methacrylic acid)). MALDI-TOF MS was conducted using a Shimadzu Axima Performance MALDI-TOF/TOF mass spectrometer, equipped with a nitrogen laser delivering 2 ns laser pulses at 337 nm with positive ion TOF detection performed using an accelerating voltage of 20 kV. Solutions in tetrahydrofuran (50 μ L) of dithranol as a matrix (saturated solution), LiCl as the cationization agent (1.0 mg mL⁻¹) and sample (1.0 mg mL⁻¹) were mixed, and 0.7 μ L of the mixture was applied to the target plate. The cyclic voltammetry measurements were done in accordance to the literature (*J. Am. Chem. Soc.*, **2008**, *130*, 10702) and recorded at 25 °C with a CHI660E potentiostat. Solutions of CuBr₂/L (1.0 mM) were prepared in dry CH₃CN containing 0.1 M Bu₄NPF₆ as the supporting electrolyte. Measurements were carried out under nitrogen at a scan rate of 0.1 V·s⁻¹ using a glassy carbon disk as the working electrode and a platinum wire as the counter electrode. Potentials were recorded versus SCE using a 0.1

M Bu₄NPF₆ salt bridge. K_{ATRP} value was estimated through correlation to Figure 2 in literature (*J. Am. Chem. Soc.*, **2008**, *130*, 10702). The gas chromatography analyses were performed using Agilent 7890A, autosampler, and a J&W Scientific DB-1701 column (30×0.25×0.25) with an FID detector. The injector and detector temperature were kept constant at 280 °C. The temperature program for the GG column was as follows: initial temperature 45 °C, 2 min; ramp 5 °C/min; final temperature 180 °C, 5 min. The UV-vis spectroscopic measurements were performed on a Shimadzu UV-2700 UV/vis spectrometer.

2. General ATRP Procedure

All polymerizations were set up and performed under an atmosphere of oxygen-free, dry argon using standard Schlenk-line techniques or inside a nitrogen-filled glovebox. In an ampule equipped with a magnetic stirrer bar, a mixture of CuBr_2 , ligand and $\text{Cu}(0)$ powder in solvent was stirred at room temperature for 2 h under the atmosphere of nitrogen. After that, monomer and initiator were added into the ampule. The ampules were placed at a certain temperature. After stirring for the allotted period of time, an aliquot (0.05 mL) was removed and quenched with CDCl_3 (0.5 mL). Conversion was determined by integration of the monomer vs. polymer resonances in the ^1H NMR spectrum of the crude product. After completion of the reaction, the contents of the ampules were dissolved in THF. The solution was filtered through a glass funnel with neutral alumina. The filtrate was concentrated under reduced pressure. The residuals were resolved with 5 mL THF. This solution was added to an approximately 50-fold excess of rapidly stirred methanol. The precipitate that formed was filtered and washed with methanol. The precipitate was dried to constant weight in a vacuum oven at 50 °C.

3. The SARA ATRP of MMA Employing Different Ligands and Initiators

Table S1. The SARA ATRP of MMA Employing Different Ligands and Initiators^a

Run	L	Initiator	t (h)	Conv. ^b (%)	$M_{n, \text{theory}}$ (kg/mol)	$M_{n, \text{GPC}}$ (kg/mol)	\bar{D}
1	SaBOX	EBiB	3.0	75	7.7	29.0	1.52
2	SaBOX	EBPA	2.3	74	7.7	30.2	1.59
3	PMDETA	EBiB	3.0	6.2	0.7	141.3	2.14
4	PMDETA	EBPA	2.3	2.9	0.4	505.3	1.56
5	Me ₆ TREN	EBiB	3.0	0	–	–	–
6	Me ₆ TREN	EBPA	2.3	0	–	–	–

^a Reaction conditions: n(MMA):n(Initiator):n(CuBr₂):n(SaBOX):n(Cu(0)) = 200:2:1:2:4, DMSO was used as the solvent (50% V_{total}), 25 °C, DP_{target} = 100. ^b Monomer conversion measured by ¹H NMR.

4. The SARA ATRP of MMA with DP_{target} = 100 in IPA/DMSO Mixed Solvent

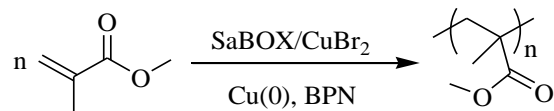
Table S2. The SARA ATRP of MMA with DP_{target} = 100 in IPA/DMSO Mixed Solvent^a

Run	IPA/DMSO (V/V)	t (h)	Conv. ^b (%)	$M_{n, \text{theory}}$ (kg/mol)	$M_{n, \text{GPC}}$ (kg/mol)	\bar{D}
1	1/1	3.0	88	8.9	15.3	1.23
2	2/1	5.0	90	9.1	16.6	1.26
3	5/1	6.0	90	9.1	15.8	1.18
4	7/1	6.5	90	9.1	11.9	1.19
5	10/1	10	88	8.9	9.2	1.17

^a Reaction conditions: n(MMA):n(BPN):n(CuBr₂):n(SaBOX):n(Cu(0)) = 200:2:1:2:4, n(MMA) = 5 mmol, IPA/DMSO was used as the solvent (50% V_{total}), 25 °C, DP_{target} = 100. ^b Monomer conversion measured by ¹H NMR.

5. First-Order Kinetic Plots as well as Evolution of MW and Đ as a Function of Monomer Conversion for ATRP of MMA

Table S3. First-Order Kinetic Study and Evolution of MW and Đ as a Function of Monomer Conversion for ATRP of MMA^a



Run	t (h)	conv. ^b (%)	$M_{n, \text{GPC}}$ (kg/mol)	$M_{n, \text{theory}}$ (kg/mol)	Đ	$\ln(C_M^0/C_M)$
1	0.5	14	2.1	1.5	1.33	0.1586
2	1	18	3.7	1.9	1.18	0.1985
3	1.5	24	4.1	2.5	1.19	0.2744
4	2	35	4.3	3.6	1.35	0.4308
5	3	48	5.4	4.9	1.40	0.6539
6	4	53	6.3	5.4	1.29	0.7550
7	5	58	5.8	5.9	1.35	0.8675
8	6	70	7.7	7.1	1.27	1.2040
9	7	81	9.7	8.2	1.28	1.6607

^a Reaction conditions: $n(\text{M}):n(\text{Initiator}):n(\text{CuBr}_2):n(\text{Ligand}):n(\text{Cu}(0)) = 200:2:1:2:4$, $n(\text{M}) = 5$ mmol, IPA/DMSO (7/1 (v/v)) was used as the solvent (50% V_{total}), 25 °C. ^b Monomer conversion measured by ¹H NMR.

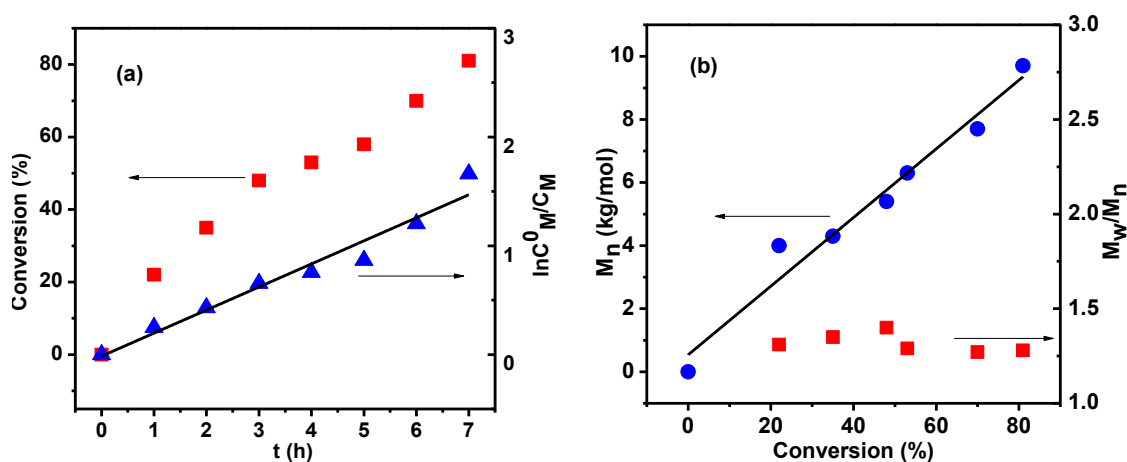


Figure S1. (a) First-order kinetic plot as well as (b) evolution of MW and Đ (M_w/M_n) as a function of conversion for ATRP of MMA employing SaBOX as the ligand (Table S2).

6. The GPC Traces of PMMA with Different DP_{target} s

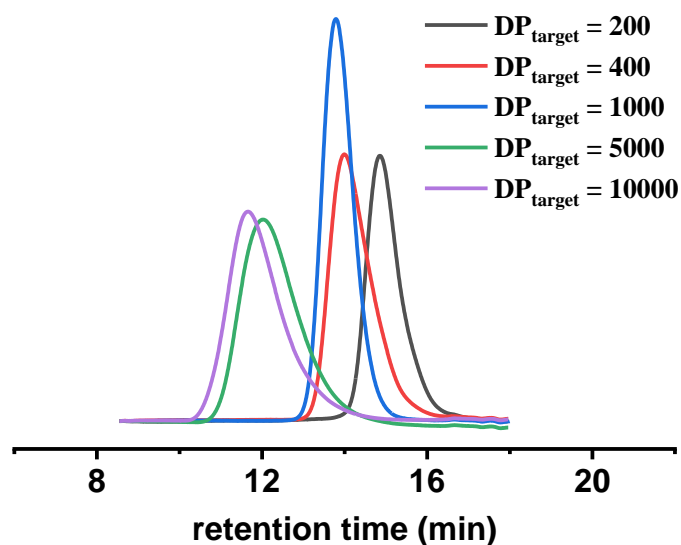


Figure S2. GPC traces of PMMA ($DP_{\text{target}} = 200\text{-}10000$, runs 5 and 7-10 in Table 2)

7. MALDI-TOF Mass Spectrum of PMMA

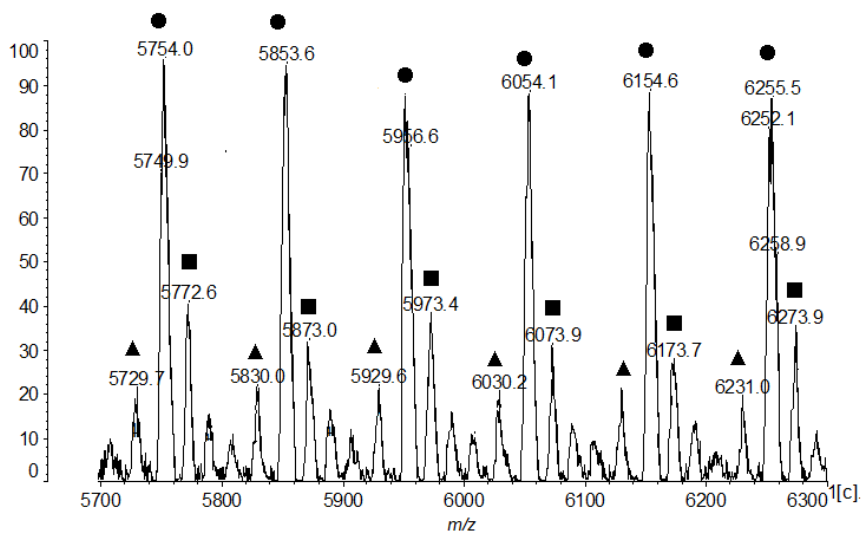


Figure S3. MALDI-TOF mass spectrum of PMMA produced by SaBOX/CuBr₂ ($M_n = 4.3$ kg/mol, $\bar{D} = 1.21$). ▲: $CN(CH_3)CH(MMA)_nBrH^+$, ●: $CN(CH_3)CH(MMA)_nBrNa^+$, ■: $CN(CH_3)CH(MMA)_nBrK^+$.

8. In Situ Chain Extension Experiments

Table S4. Conversion and MW Analysis of the in situ Chain Extension of Poly(methyl methacrylate)

Run	Block	DP _{target}	t (h)	Conv. (%) ^c	M _{n, GPC} (kg/mol)	M _{n,theory} (kg/mol)	Đ
1 ^a	MMA	50	16	>99	7.0	5.1	1.21
2 ^b	MMA-MMA	50	8	75	13.2	8.8	1.12

^a Reaction conditions: n(MMA):n(BPN):n(CuBr₂):n(SaBOX):n(Cu(0)) = DP_{target}:1:0.5:1:2, n(MMA) = 2.5 mmol, IPA/DMSO (7/1 (v/v)) was used as the solvent (50% V_{total}), 25 °C. ^b in situ adding MMA and solvent with a ratio of 1:1 (V/V). ^c Monomer conversion measured by ¹H NMR.

Table S5. The Synthesis of PMMA-*b*-P*n*BMA via in situ Chain Extension

Run	Block	DP _{target}	t (h)	Conv. (%) ^c	M _{n, GPC} (kg/mol)	M _{n,theory} (kg/mol)	Đ
1 ^a	MMA	50	15	99	7.3	5.1	1.17
2 ^b	MMA- <i>n</i> BMA	50	12	86	13.0	11.2	1.15

^a Reaction conditions: n(MMA):n(BPN):n(CuBr₂):n(SaBOX):n(Cu(0)) = DP_{target}:1:0.5:1:2, n(MMA) = 2.5 mmol, IPA/DMSO (7/1 (v/v)) was used as the solvent (50% V_{total}), 25 °C. ^b in situ adding *n*BMA and solvent with a ratio of 1:1 (V/V). ^c Monomer conversion measured by ¹H NMR.

9. The Determinations of Equilibrium Constant and Activation Rate Constant

$$F(Y) = \left(\frac{I_0 C_0}{C_0 - I_0} \right)^2 \left(\frac{1}{C_0^2 (I_0 - Y)} + \frac{2}{I_0 C_0 (C_0 - I_0)} \ln \left(\frac{I_0 - Y}{C_0 - Y} \right) + \frac{1}{I_0^2 (C_0 - Y)} \right)$$

Equation S1. Modified Fischer's Equation

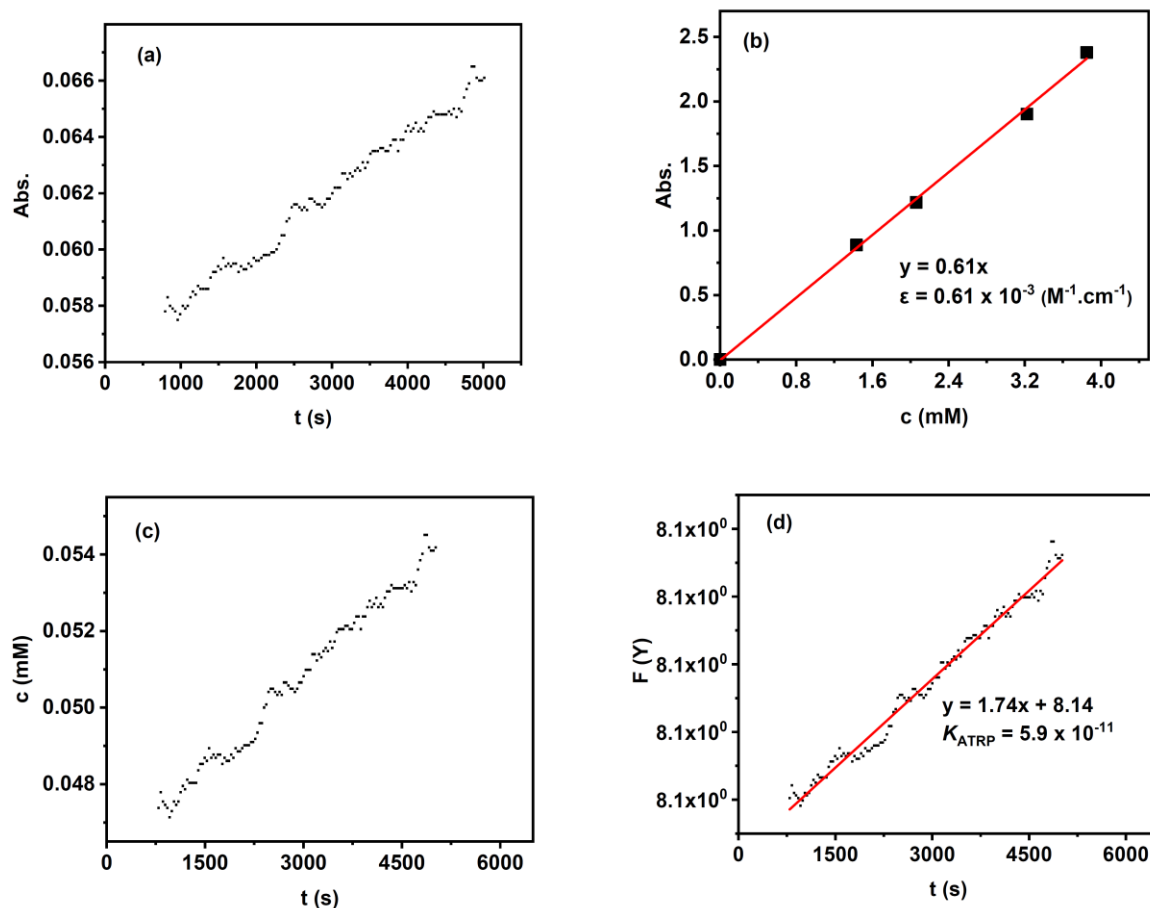


Figure S4. (a) The absorbancy of Cu(II) species varying with time; (b) The determination of absorption coefficient; (c) The concentration of Cu(II) species varying with time; (d) Experiment for the determination of K_{ATRP} via new equations ($F(Y)$ vs t): $[\text{CuBr}]_0 = [\text{SaBOX}]_0 = 5 \text{ mM}$, $[\text{EBiB}]_0 = 500 \text{ mM}$; Solvent = MeCN; temperature = $25 \pm 2 \text{ }^\circ\text{C}$.

$$\text{pseudo-1}^{\text{st}}\text{-order: } \left[\frac{\text{Cu}^{\text{I}}\text{Y}}{\text{L}_n} \right]_0 \gg [\text{R-X}]_0$$

$$-\frac{d\ln[\text{R-X}]}{dt} = \text{slope} = k_{\text{app}}[\text{Cu}^{\text{I}}\text{Y}/\text{L}_n]_0 = k_a[\text{Cu}^{\text{I}}\text{Y}/\text{L}_n]_{\text{act}}$$

Equation S2. Pseudo-first-order Equation

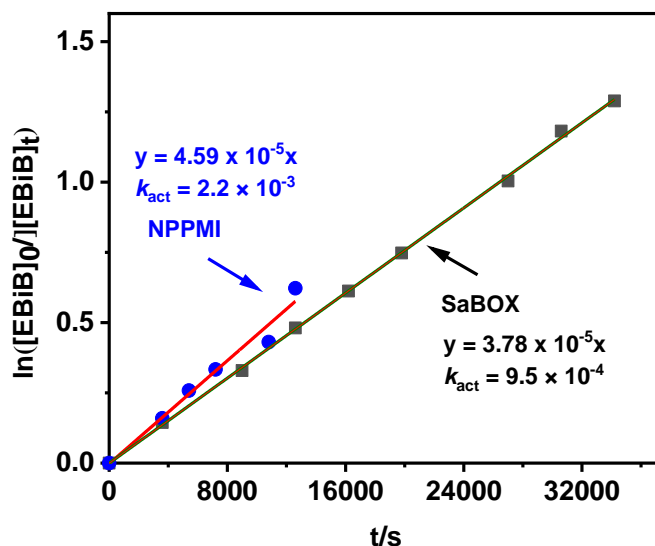


Figure S5. Pseudo-first-order kinetic plot of the activation process for SaBOX and NPPMI in acetonitrile at 35 °C; $[\text{CuBr}]_0/[\text{EBiB}]_0/[\text{TEMPO}]_0/[\text{TCB}]_0 = 20/1/10/2$, $[\text{CuBr}]_0 = [\text{Ligand}]_0 = 40 \text{ mM}$.

Table S6. Experimental Determination of activation rate constants^a

Run	Ligand	Slope (10^{-5} S^{-1})	k_{app} ($\text{M}^{-1} \cdot \text{S}^{-1}$)	k_{act} ($\text{M}^{-1} \cdot \text{S}^{-1}$)
1	NPPMI	4.59	1.1×10^{-3}	2.2×10^{-3}
2	SaBOX	3.78	9.5×10^{-4}	9.5×10^{-4}

^a Conditions: $[\text{CuBr}]_0/[\text{EBiB}]_0/[\text{TEMPO}]_0/[\text{TCB}]_0 = 20/1/10/2$, $[\text{CuBr}]_0 = [\text{Ligand}]_0 = 40 \text{ mM}$; Solvent = MeCN; temperature = $35 \pm 2 \text{ }^\circ\text{C}$.

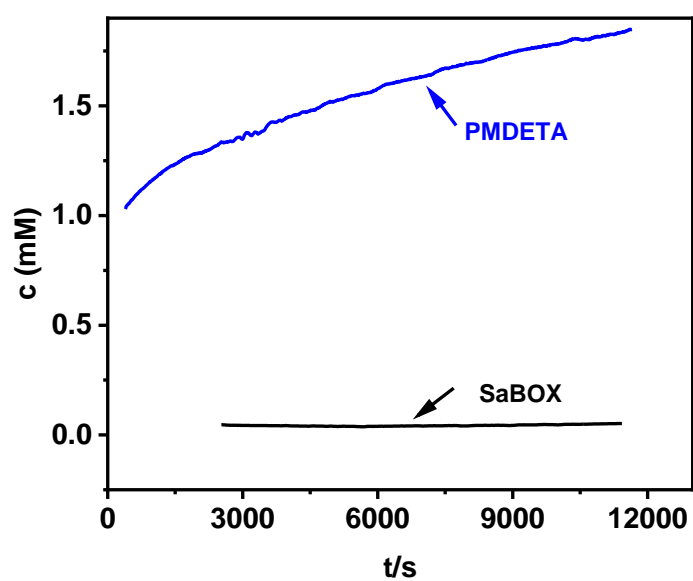


Figure S6. The evolution of Cu(II) species by the UV-vis spectrometric experiments: $[\text{CuBr}]_0 = [\text{Ligand}]_0 = [\text{BPN}]_0 = 5 \text{ mM}$; Solvent = MeCN; temperature = $25 \pm 2 \text{ }^\circ\text{C}$.